DOI: 10.1002/cphc.200((will be filled in by the editorial staff))

Polyoxovanadate as Advanced Electrode Material for Supercapacitors

Han-Yi Chen,[a,b] Grace Wee, [b,c] Rami Al-Oweini,[d] Jochen Friedl,[a,e] Kim Soon Tan,[b] Yuxi Wang,[a] Chui Ling Wong,[b,c] Ulrich Kortz,[d] Ulrich Stimming*,[a,e,f] and Madhavi Srinivasan*[a,b,c]

A polyoxovanadate, $Na_6V_{10}O_{28}$, is investigated for the first time as electrode material for supercapacitors in this work. The electrochemical properties of $Na_6V_{10}O_{28}$ electrodes are studied in Li-ion containing organic electrolyte (1 M $LiClO_4$ in propylene carbonate) by galvanostatic charge/discharge and cyclic voltammetry in three-electrode configuration. $Na_6V_{10}O_{28}$ electrodes exhibit high specific capacitance up to 354 F g^{-1}. An asymmetric supercapacitor using activated carbon (AC) as positive electrode and $Na_6V_{10}O_{28}$ as negative electrode is fabricated and exhibits a high energy density of 73 Wh kg^{-1} with a power density of 312 W kg^{-1}, which successfully demonstrates that $Na_6V_{10}O_{28}$ is a promising electrode material for high energy supercapacitor applications.

Introduction

In contrast to batteries which usually have high energy density but low power density, SCs have the advantage of delivering high power density which leads to ~100x faster charge/discharge rates than batteries.[1] Besides, SCs also possess high cycle life with good stability. Therefore, they can be used to complement or replace batteries in some energy storage applications, such as load levelling and uninterruptible power supplies.

Presently, activated carbon (AC) is the most commonly used electrode material in commercial SCs.[2] Its high surface area grants a high double layer capacitance. However, limited charge storage capability of activated carbon has caused current SCs to suffer from low energy density (~20x lower than batteries), which hinders their widespread usage, especially for applications such as electric vehicles and smart grid implementation. Hence, the invention of electrode materials with high energy density and at the same time rapid charge/discharge capability is needed for better usage in hybrid vehicles and smart grid applications.

The utilization of transition metal oxides (TMOs) such as ruthenium oxide,[3] vanadium oxide,[4, 5] manganese oxide,[6] indium oxide,[7] and tin oxide has been widely investigated for improving the energy density of SCs.[8] These oxides are redox-active materials that can be used to construct pseudocapacitors and store electrochemical charge within highly reversible surface redox reactions. Some of these TMOs exhibit high specific capacitance, but their power densities are much lower than carbon materials.[9-12]

Polyoxometalates (POMs) are transition metal oxide clusters with fast and reversible multi-electron redox reactions,[13-17] and were reported to possess high capability for charge storage in batteries and capacitors.[1, 3, 18, 19] However, only a few POM materials were studied in SCs[19-26], and most of them were combined with carbon materials such as carbon nanotubes (CNTs),[23, 25] active carbon,[26] or conducting polymers such as polyaniline (PAni),[22] poly(3, 4-ethylenedioxythiophene) (PEDOT),[21] poly(diallyldimethylammonium) chloride (PDDA),[25] and pyrrole (PPy)[20] to enhance the energy storage capabilities with the multi-electron redox reactions of POM materials. V. Ruiz et al. prepared an AC/$H_3PMo_{12}O_{40}$ hybrid material by simple adsorption of the POM onto the surface of activated carbon for symmetric SCs, providing specific capacitance of 183 F g^{-1} at a current density of 2 A g^{-1}.[26] CNTs/$Cs_xPM_{O12}O_{40}$ hybrid materials as electrode materials for symmetric SCs have been studied by K. Cuentas-Gallegos et al., showing high specific capacitance of 285 F g^{-1} and high energy density of 57 Wh kg^{-1} at a current density of 0.2 A g^{-1}, but only 20 F g^{-1} and energy density of 12.5 Wh kg^{-1} at current density of 2 A g^{-1}.[23] G. M. Suppes et al. reported an asymmetric SC with PPy/$H_3PMo_{12}O_{40}$ as positive electrode and PEDOT/$H_3PW_{12}O_{40}$ as negative electrode in 0.5 M H_2SO_4 aqueous electrolyte, which exhibited device capacitance of 31 F g^{-1} with a maximum

[a] *H.-Y. Chen, J. Friedl, Dr. Y. Wang, Prof. U. Stimming*, and Prof. M. Srinivasan*
TUM CREATE
1 CREATE Way, #10-02 CREATE Tower, Singapore
E-mail: ulrich.stimming@tum-create.edu.sg, madhavi@ntu.edu.sg*
[b] *H.-Y. Chen, Dr. G. Wee, K. S. Tan, C. L. Wong, Prof. M. Srinivasan*
School of Materials Science and Engineering Nanyang Technological University, Singapore
[c] *Dr. G. Wee, Dr. C. L. Wong, Prof. M. Srinivasan*
Energy Research Institute @ NTU (ERI@N)
Research Techno Plaza, 50 Nanyang Drive, Singapore 637553
[d] *Dr. R. Al-Oweini, Prof. U. Kortz*
School of Engineering and Science, Jacobs University
P.O. Box 750561, 28725 Bremen, Germany
[e] *J. Friedl, Prof. U. Stimming*
Department of Physics E19, Technische Universität München
James-Franck Str. 1, 85748 Garching, Germany
[f] *Prof. U. Stimming*
Institute for Advanced Study (IAS) of the Technische Universität München
Lichtenbergstr. 2a, 85748 Garching, Germany*

energy density of 4 Wh kg^{-1} and power density of 103 W kg^{-1}. [24]

In this study, we present for the first time the utilization of the vanadium-based POM material decavanadate(V), $Na_6V_{10}O_{28}$ as electrode material in SCs. Based on the performance of transition metal oxides, V_2O_5 provide relatively high specific capacitance due to the multiple oxidation states (V^{2+}~V^{5+}). Hence, vanadium-based POMs are identified as potential electrode materials which might provide high specific capacitance and high energy density of SCs in this study.[11, 27] The electrochemical properties of decavanadate electrodes are investigated by electrochemical measurements such as galvanostatic charge/discharge and cyclic voltammetry. Furthermore, an asymmetric SC device which combines $Na_6V_{10}O_{28}$ as negative electrode and commercial activated carbon (AC) as positive electrode is fabricated to demonstrate the potential for SC applications. Besides, most of the POM SCs employ acidic aqueous electrolyte, which limits the operating voltage of the SC to roughly 1 V.[28] In order to achieve high energy density and power density, a Li-ion-containing organic electrolyte (1 M $LiClO_4$ in propylene carbonate (PC)) is employed to extend the potential window.

Results and Discussion

Material characterization of $Na_6V_{10}O_{28}$

The sodium salt of the decavanadate polyanion is characterized by FTIR and ^{51}V NMR. Figure 1a shows the FTIR spectrum in which the characteristic absorption bands of $Na_6V_{10}O_{28}$ are detected. The vibrational mode centered at 956 cm^{-1} is attributed to a V=O bond.[29] The bands located at 837, 746, and 576 cm^{-1} are assigned to V-O-V bridging as reported for decavanadate in previous studies.[29] In solution, the vanadium atoms in the decameric vanadate species can also be detected by ^{51}V NMR. The spectrum obtained in Figure 1b shows the characteristic signals of $[V_{10}O_{28}]^{6-}$ (−514 ppm, −500 ppm, −424 ppm) which are similar to previous studies.[30, 31] The inset of Figure 1b shows the polyhedral representation of decavanadate.

A Brunauer-Emmett-Teller (BET) surface area of 21 m^2 g^{-1} is obtained for $Na_6V_{10}O_{28}$ by N_2 adsorption-desorption isotherms shown in Figure 1c. From the Barrett-Joyner-Halenda (BJH) pore size distribution, as shown in the inset of Figure 1c, the pore diameters of $Na_6V_{10}O_{28}$ show as size distribution ranging from ~ 3 nm to ~ 160 nm, and most of these pores show a narrower distribution of mesopores centered between 3 and 5 nm.

Figure 2a shows a scanning electron microscopy (SEM) image of powder $Na_6V_{10}O_{28}$. The morphological structure of $Na_6V_{10}O_{28}$ is micro-sized rods with a diameter of 0.5–1 μm and a length of several micrometers. To further investigate the structure and crystallinity of $Na_6V_{10}O_{28}$ rods, a transmission electron microscope (TEM) is used. Figure 2b shows a bright-field TEM image of a $Na_6V_{10}O_{28}$ rod with a diameter of about 600 nm. The high resolution transmission electron microscopy (HRTEM) image of an individual rod (Figure 2c) provides further insight into the structure. The $Na_6V_{10}O_{28}$ rod exhibits polycrystallinity in random orientation with d-spacings of 0.769 nm and 0.333 nm which are consistent with JCPDS data file 79-1787.

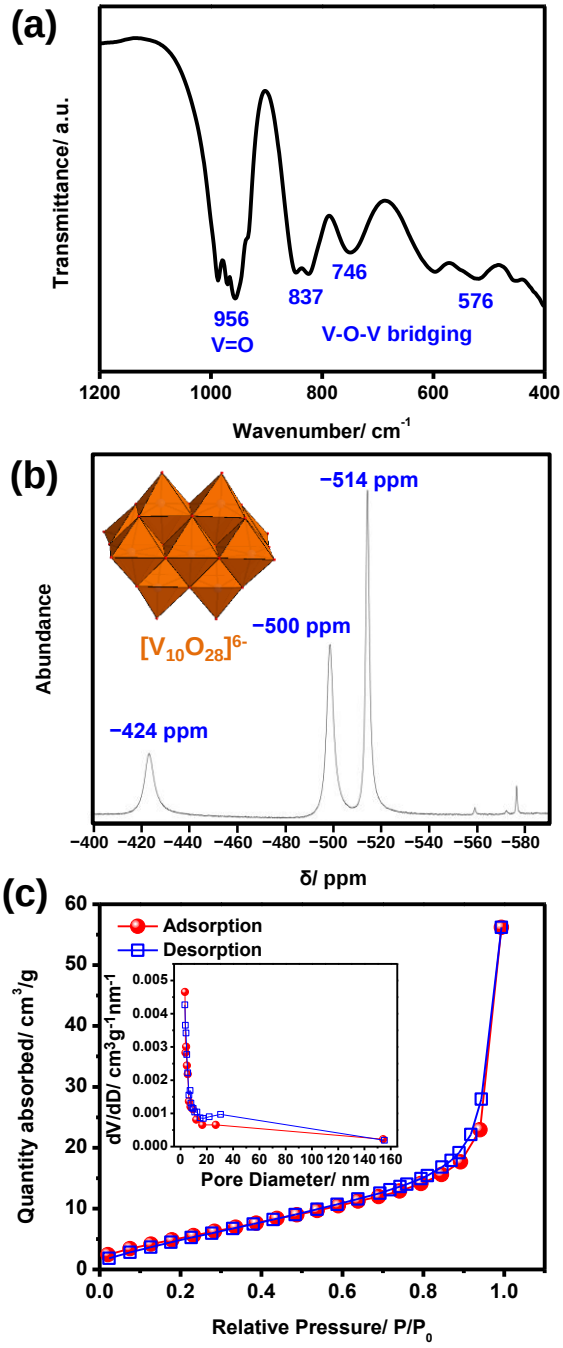

Figure 1. (a) FTIR spectrum, (b) ^{51}V NMR spectrum, and (c) BET graph of $Na_6V_{10}O_{28}$. Inset in (b) is the polyhedral representation of $[V_{10}O_{28}]^{6-}$, color code: VO_6. Inset in (c) is the corresponding BJH pore size distribution curve for $Na_6V_{10}O_{28}$ determined by N_2 adsorption-desorption isotherms

Electrochemical characterization of $Na_6V_{10}O_{28}$

Electrochemical properties of $Na_6V_{10}O_{28}$ electrodes in three-electrode configuration

To investigate the electrochemical performance of $Na_6V_{10}O_{28}$ as electrode material for SCs in 1 M $LiClO_4$ in PC, three-

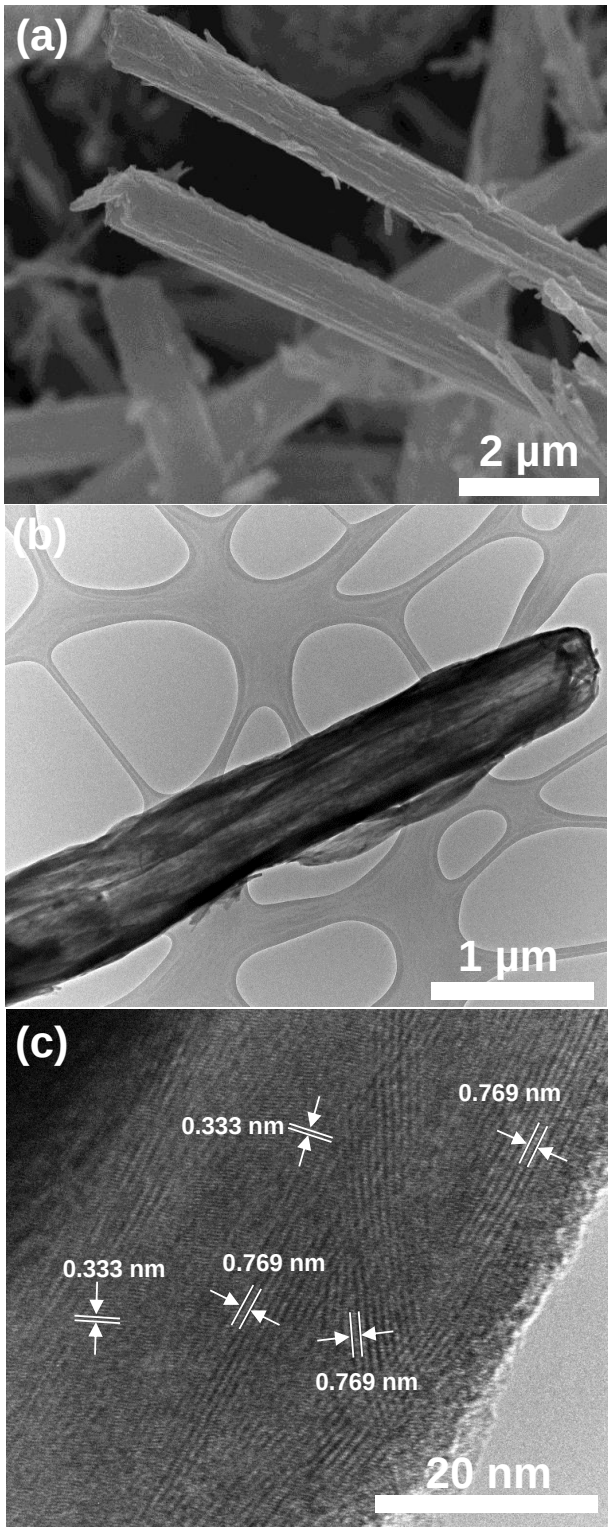

Figure 2. (a) The SEM image of $Na_6V_{10}O_{28}$ powder (b) A bright-field TEM image of a $Na_6V_{10}O_{28}$ rod (c) A high-resolution TEM image

electrode CV and galvanostatic charge/discharge measurements were conducted. A Pt wire served as counter electrode and $Ag/AgNO_3$ reference electrode was used (approximately 0.55 V vs. NHE,[32] supporting electrolyte for reference electrode is 0.1 M tetraethylammonium tetrafluoroborate ($TEABF_4$) and 0.01 M $AgNO_3$ in acetonitrile). All potentials are given vs. this reference electrode. Figure 3a shows CV curves of a $Na_6V_{10}O_{28}$ electrode measured from −1.6 V to 1.2 V at various scan rates (20, 10, 5, and 2 mV s^{-1}). The CV curves deviate from the rectangular shape of an ideal capacitor which indicates faradaic processes.[23] The redox peaks are broader at higher scan rates indicating slower kinetics.[26] At 2 mV s^{-1}, oxidation peaks can be observed at -0.17 V and 0.45 V, corresponding reduction peaks at −0.78 V, −0.53 V, −0.02 V and 0.37 V. These peaks result from the redox transition of vanadium ions and intercalation or adsorption of Li^+ ions into the $Na_6V_{10}O_{28}$ structure. The evidence for this claim will be provided later. Figure 3b shows the gravimetric specific capacitance of $Na_6V_{10}O_{28}$ electrodes calculated from CV curves at different scan rates. The specific capacitances from the CV curves are calculated using the following equation:[33]

$$C_{sp} = \frac{\int i\Delta t}{\Delta U \times m} = \frac{q}{\Delta U \times m} \quad (1)$$

where C_{sp} is the gravimetric specific capacitance (F g^{-1}), q is the charge obtained by integrating the negative currents (discharging cycle) after subtracted the charge from current collector, ΔU is the potential range (V), and m is the mass of the active materials on the electrodes (g). From the CV curves of $Na_6V_{10}O_{28}$ electrodes, the specific capacitance of 121, 142, 170, and 223 F g^{-1} are obtained for 20, 10, 5, and 2 mV s^{-1}, respectively. This large spread indicates slow kinetics.

As shown in Figure 3c and 3d, specific capacitances are also obtained by employing galvanostatic charge/discharge measurements from −1.6 V to 1.2 V at current densities ranging from 10 to 0.1 A g^{-1}. The nonlinear charge/discharge profile indicates the pseudocapacitive behavior, and the potential positions of the plateaus are similar with the redox peaks observed in the CV curves. The specific capacitance is calculated by equation:[34]

$$C_{sp} = \frac{I \times \Delta t}{m \times \Delta U} \quad (2)$$

where I is the constant current (A), and Δt is discharge time (s), respectively. The specific capacitance of $Na_6V_{10}O_{28}$ electrodes obtained from galvanostatic charge/discharge at current density of 10, 5, 2, 1, 0.5, and 0.1 A g^{-1} are 87, 111, 143, 172, 189, and 354 F g^{-1}, respectively. According to Figure 3b and 3d, the decrease of the specific capacitance with increasing scan rate and current density can be interpreted such that (1) Low electrical conductivity of thick $Na_6V_{10}O_{28}$ electrode (~ 40 $\boldsymbol{\mu}$m) results in a large ohmic drop during fast charging and discharging.[1, 27] (2) Slow diffusion of Li^+ ion into the pores of $Na_6V_{10}O_{28}$. At high scan rate and high current density, the charge storage only occurs at the outer active surface due to the limitation of Li^+ ion diffusion. On the other hand, at low scan rate and low current density, all the active surface area can be used to store charge which in turn provides higher specific capacitance.[1, 11]

To further investigate the redox behavior of $Na_6V_{10}O_{28}$ electrodes during charge–discharge process in 1 M $LiClO_4$ organic electrolyte, X-ray photoelectron spectroscopy (XPS) is performed. Figure 4a shows the XPS spectra of V $2p_{3/2}$ and Li 1s of $Na_6V_{10}O_{28}$ electrodes at 0.7 V (charged) and −1.3 V (discharged). The background curves are corrected in order to compare the concentration of V and Li.

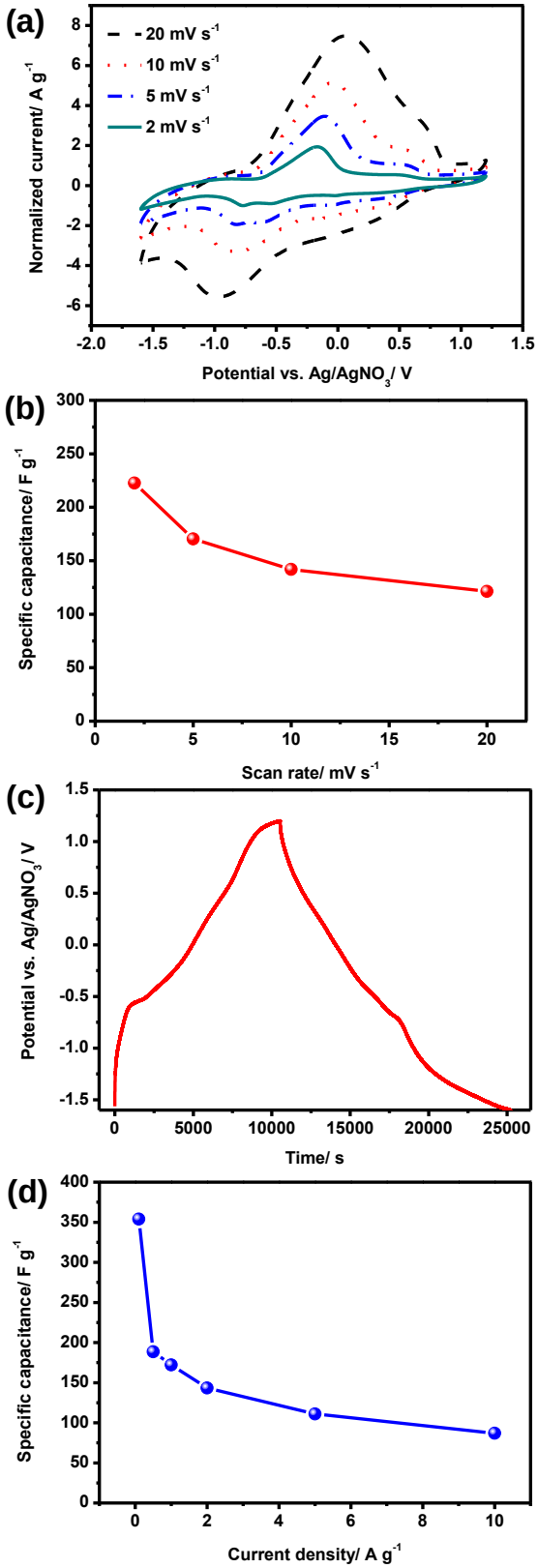

Figure 3. Electrochemical characterizations of $Na_6V_{10}O_{28}$ electrodes in 1 M $LiClO_4$/PC in a three-electrode configuration with Pt wire as the counter electrode and $Ag/AgNO_3$ as the reference electrode: (a) cyclic voltammograms and (b) the specific capacitance at various scan rates (20, 10, 5, and 2 mV s^{-1}); (c) galvanostatic charge-discharge curves at current density of 0.1 A g^{-1}, and (d) the specific capacitance at various current densities (10, 5, 2, 1, 0.5, and 0.1 A g^{-1}).

The V $2p_{3/2}$ XPS spectra are recorded to determine the change in the oxidation state of V. It is found in the literature that V^{5+} has a $2p_{3/2}$ binding energy of ~517.3 eV, while V^{4+} has a binding energy of ~516.2 eV for $VO_x•H_2O$.[35] As shown in Figure 4a, a pair of peaks located at 517.1 eV and 516 eV with peak splitting of 1.1 eV reveal the partial reduction of V^{5+} to V^{4+} which corresponds with the literature.[35] The concentration of V^{4+} increases after discharging from 0.7 V to −1.3 V, indicating the redox process during the discharge process. The fact that the increased amount of V^{4+} is not large might be due to the air contact that causes re-oxidation during electrode transportation to the ex-situ XPS measurement. Furthermore, the XPS spectra of Li 1s are detected as shown in Figure 4a. The concentration of Li increases during discharge process. This can be attributed to Li intercalation into or Li adsorption onto the $Na_6V_{10}O_{28}$ electrode.[36] The changing presence of Li and reduction of V^{5+} to V^{4+} indicates simultaneous intercalation and/or adsorption during the V reduction processes.

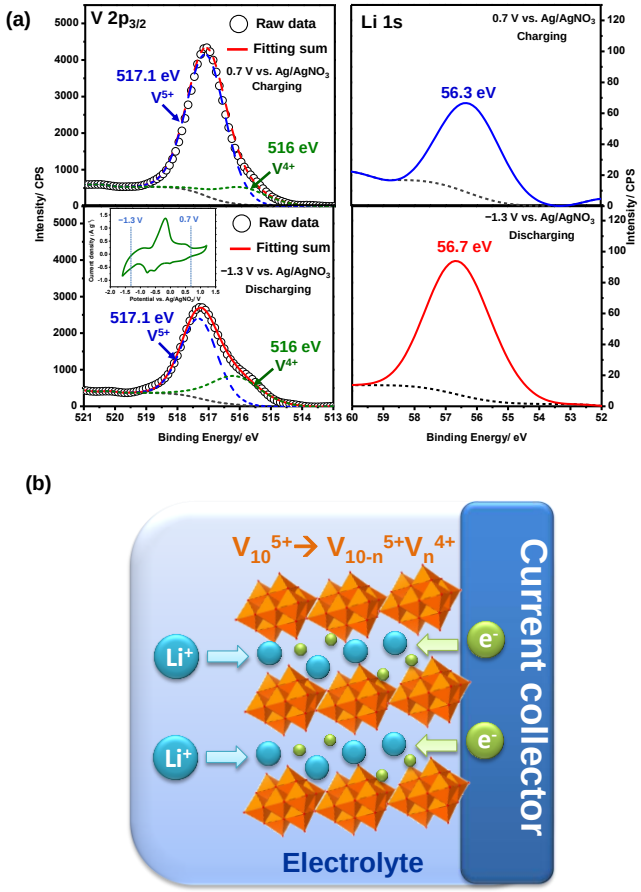

Figure 4. XPS spectra of (a) V $2p_{3/2}$ and Li 1s after the charge discharged cycle of $Na_6V_{10}O_{28}$ electrodes tested in 1 M $LiClO_4$/PC. (b) A schematic diagram showing the Li ion intercalation and/or adsorption process in $Na_6V_{10}O_{28}$ electrodes.

Based on the findings from XPS spectra, the charge storage mechanism of $Na_6V_{10}O_{28}$ electrodes in lithium ion based organic electrolyte is dominated by the redox processes accompanied by insertion/extraction and/or desorption/adsorption processes of lithium ion from the electrolyte as given below:

$$Na_6V_{10}O_{28} + \mathrm{n}Li^+ + \mathrm{n}e^- \leftrightarrow Li_{\mathrm{n}}Na_6V^{5+}_{10-\mathrm{n}}V^{4+}_{\mathrm{n}}O_{28} \quad (3)$$

This reaction provides high faradic pseudocapacitance (357 F g^{-1} at a current density of 0.1 A g^{-1}) when intercalating and/or adsorbting Li^+ ions with partial reduction of V^{5+} to V^{4+} during discharge process as shown in Figure 4b.

Asymmetric supercapacitor based on $Na_6V_{10}O_{28}$ and activated carbon

To demonstrate the potential of $Na_6V_{10}O_{28}$ electrodes for actual device applications, asymmetric SCs are assembled using $Na_6V_{10}O_{28}$ as the negative electrode and AC as the positive electrode in $LiClO_4$-containing organic electrolyte. During the charging process, ClO_4^{-1} ions are adsorbed onto the porous structure of AC (positive electrode), while Li ions are intercalated into or adsorbed onto the $Na_6V_{10}O_{28}$ (negative electrode) with partial reduction of V^{5+} to V^{4+}. Discharging process is opposite to the charge process.

In order to obtain the maximum gravimetric cell energy of asymmetric SCs, the voltage range and the mass ratio are optimized. Figure 5a shows the CV curves of AC, $Na_6V_{10}O_{28}$, and blank substrate (graphite paper) at 10 mV s^{-1} in three-electrode configuration. The CV curve of AC reveals a near-ideal rectangular shape, illustrating almost pure electrochemical double layer charging. The potential regions of AC as positive electrode and $Na_6V_{10}O_{28}$ as negative electrode were located between −1.6 V to 1.2 V vs. $Ag/AgNO_3$, so the performance of asymmetric SCs is tested in the voltage window of 0 V to 2.8 V. The mass ratio is optimized according to the equation $q_+ = q_- \left(C_{sp+}m_+\Delta U_+ = C_{sp-}m_-\Delta U_-\right)$, where + represents positive electrode, − represents negative electrode.[27, 37] The specific capacitances of AC and $Na_6V_{10}O_{28}$ are calculated at a scan rate of 10 mV s^{-1} from the CV curves (after subtracting the blank capacitance of graphite paper) in Figure 5a. They were 109 and 142 F g^{-1}, respectively. According to these data, an optimized mass ratio of AC : $Na_6V_{10}O_{28}$ = 1.3 : 1 is selected in this work.

The electrochemical performance of AC//$Na_6V_{10}O_{28}$ asymmetric SC with the optimized mass ratio of 1.3 : 1 in the voltage window of 0 V to 2.8 V is shown in Figure 5b and Figure 6. Figure 5b shows the CV curves in different scan rates (20, 10, 5, and 1 mV s^{-1}). The CV curves of the AC//$Na_6V_{10}O_{28}$ asymmetric SC deviate from an ideal rectangular shape. This indicates that in the asymmetric device which features AC as one of the electrode materials, faradaic reactions add pseudocapacitance to the capacitance stemming from the electrochemical double layer.[37]

Figure 6a shows the galvanostatic charge/discharge profile at current densities of 0.5 A g^{-1} (mass based on the negative electrode). It is worth mentioning that the slopes of the charge/discharge curves are not strictly linear indicating that electrochemical performance of the AC//$Na_6V_{10}O_{28}$ asymmetric SC is a combination of double-layer capacitance and pseudocapacitance.[37] The specific capacitance (C_{sp}) of the asymmetric and symmetric SCs can be calculated by using the following equation.[38]

$$C_{sp} = \frac{2C_e}{m} \quad (4)$$

where m is the mass of the active materials in negative electrode (g), and C_e is the experimental capacitance measured from the following equation.[38]

$$C_e = \frac{I \times \Delta t}{\Delta U} \quad (5)$$

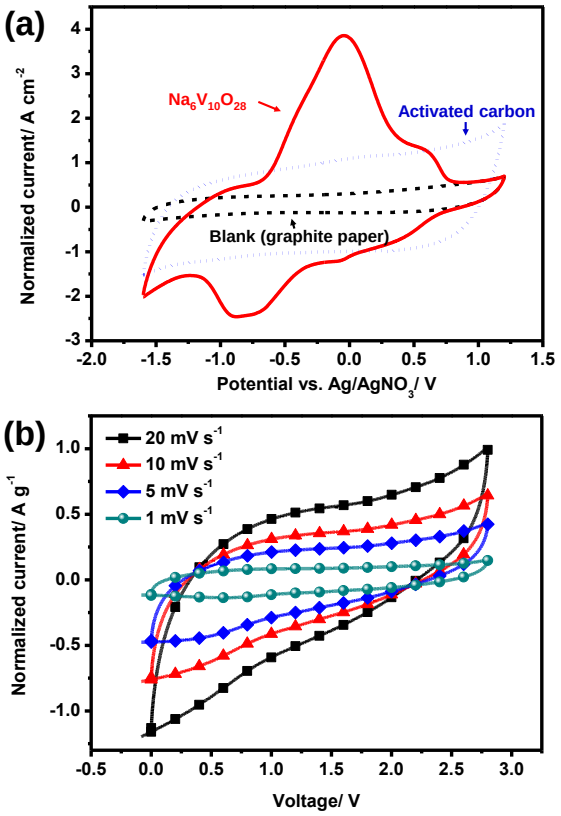

Figure 5. (a) Cyclic voltammograms of AC, $Na_6V_{10}O_{28}$, and blank electrode (graphite paper) measured at 10 mV s^{-1} in three-electrode configuration. (b) Cyclic voltammograms of AC//$Na_6V_{10}O_{28}$ asymmetric SC at the mass ratio of m_+/m_-=1.3 : 1 in various scan rates (20, 10, 5, 1 mV s^{-1}).

Figure 6b and 6c compare the specific capacitance and Ragone plots of AC//$Na_6V_{10}O_{28}$ asymmetric SC and AC//AC symmetric SC at various current densities. The AC//$Na_6V_{10}O_{28}$ asymmetric SC delivers the specific capacitance of 80, 104, 152, 203, and 269 F g^{-1} at current densities of 10, 5, 2, 1, and 0.5 A g^{-1}, respectively. These values are significantly higher than for the AC//AC symmetric SC. As expected, the specific capacitances are smaller at high current densities for both AC//$Na_6V_{10}O_{28}$ asymmetric SC and AC//AC symmetric SC.[22] A detailed analysis of AC//AC symmetric SC will not be discussed in this paper. However, the reduction of the specific capacitance of AC//AC symmetric SC at higher current density is mainly due to the mass transfer limitation of Li^+ ions inside porous AC structure.[1, 39] For AC//$Na_6V_{10}O_{28}$ asymmetric SC, the specific capacitance diminishes even more drastically with increasing current density, which either results from the

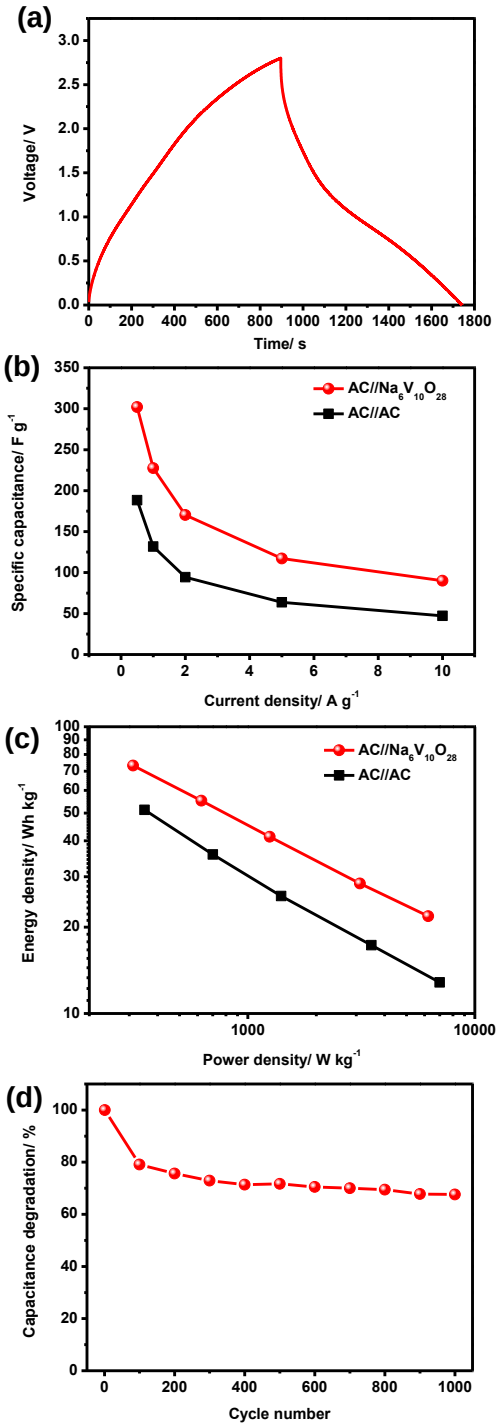

Figure 6. Electrochemical performance of AC//$Na_6V_{10}O_{28}$ asymmetric SC at the mass ratio of m_+/m_-=1.3 : 1. (a) Galvanostatic charge-discharge curves at different current densities of 0.5-10 A g^{-1}. (b) The specific capacitance and (c) the Ragone plots of the AC//$Na_6V_{10}O_{28}$ asymmetric SC and AC//AC symmetric SC as contrast at various current densities of 0.5-10 A g^{-1}. (d) Capacitance degradation of AC//$Na_6V_{10}O_{28}$ asymmetric SC at 1 A g^{-1}.

relatively low electrical conductivity of $Na_6V_{10}O_{28}$ or from the kinetics of the redox-reactions which are not fast enough to cope with the high rates.[1] Energy and power densities at different current densities for the two devices are plotted as a Ragone plot in Figure 6c. Energy and average power densities obtained during the discharge are calculated from the following relations: [27, 37]

$$E = \frac{1}{2}\frac{C_e}{M}\Delta U^2 \quad (6)$$

$$P = \frac{\mathrm{E}}{\Delta \mathrm{t}} \quad (7)$$

where M is the total mass of the active material in both negative and positive electrodes. It can be observed that both energy density and power density of the AC//$Na_6V_{10}O_{28}$ asymmetric SC are much higher than the AC//AC symmetric SC. The maximum energy density of 73 Wh kg^{-1} can be achieved from the AC//$Na_6V_{10}O_{28}$ asymmetric SC with a power density of 312 W kg^{-1}, while the energy density of AC//AC symmetric SC is around 51 Wh kg^{-1} with similar power density. Even at the power density of 6238 W kg^{-1}, the energy density of AC//$Na_6V_{10}O_{28}$ asymmetric SC still provides a higher energy density of 22 Wh kg^{-1} than the AC//AC symmetric SC (around 13 Wh kg^{-1}), demonstrating that $Na_6V_{10}O_{28}$ in organic electrolyte is promising for SC applications. For ~~a~~ commercial ~~supercapacitor~~SCs, ~~the~~ energy and power ~~densities~~ densitiy are determined by using the total mass of the device. ~~As comparison~~Therefore, we ~~apply~~ use the total mass of the device~~s~~ including both electrodes, current collectors, electrolyte, and separator ~~in the calculation~~to determine device-specific values. The maximum device energy density of 0.8 Wh kg^{-1} can be achieved with a device power density of 3.4 W kg^{-1}, and a device power density of 67.5 W kg^{-1} with a device energy density of 0.24 Wh kg^{-1} from the AC//$Na_6V_{10}O_{28}$ asymmetric SC.

Figure 6d illustrates the capacitance degradation of an AC//$Na_6V_{10}O_{28}$ asymmetric SC measured between 0 and 2.8 V with cycle charge-discharge test at 1 A g^{-1}. After the initial decrease of about 20 % in the first 100 cycles the further decrease was slow with ~ 1 % per 100 cycles. After 1000 cycles, the AC//$Na_6V_{10}O_{28}$ asymmetric SC exhibited moderate cycle stability with capacitance retention around 70 %.

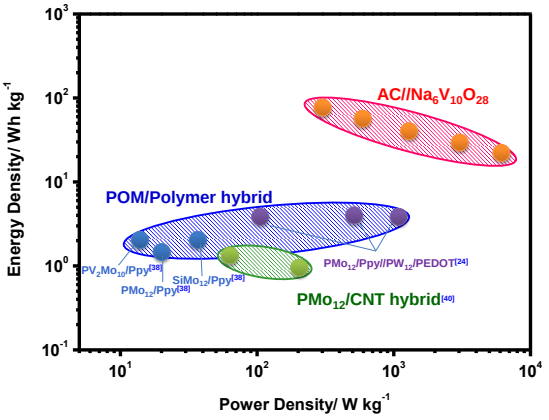

Figure 7. The Ragone plot of AC//$Na_6V_{10}O_{28}$ asymmetric supercapacitor compared with other POM SCs.[24, 38, 40] (PMo_{12}: $H_3PMo_{12}O_{40}$, $SiMo_{12}$: $H_4SiMo_{12}O_{40}$, PV_2Mo_{10}: $H_5PV_2Mo_{10}O_{40}$, PW_{12}: $H_3PW_{12}O_{40}$)

Figure 7 summarizes the energy density and power density of AC//$Na_6V_{10}O_{28}$ asymmetric SC developed in this work and compares it to other POM/polymer or POM/CNT hybrid SCs.[24, 38, 40] Compared to other POM SC, the AC//$Na_6V_{10}O_{28}$ asymmetric SC in this study exhibits the highest energy density and power density in 1 M $LiClO_4$ in PC demonstrating $Na_6V_{10}O_{28}$ is a promising electrode material for SC applications.

Conclusion

A polyoxovanadate, $Na_6V_{10}O_{28}$, has been demonstrated to be a promising electrode material for SC applications. The electrochemical properties of $Na_6V_{10}O_{28}$ electrodes in Li-ion containing organic solution (1 M $LiClO_4$ in PC) have been studied in three-electrode configuration. The electrodes exhibit a maximum specific capacitance of 354 F g^{-1} at 0.1 A g^{-1}. Furthermore, an asymmetric SC device comprising $Na_6V_{10}O_{28}$ as negative electrode and commercial activated carbon (AC) as positive electrode is successfully fabricated and studied for the first time. The AC//$Na_6V_{10}O_{28}$ asymmetric SC exhibits high energy density of 73 Wh kg^{-1} with the power density of 312 W kg^{-1}, and high power density of 6238 W kg^{-1} with the energy density of 22 Wh kg^{-1}, which are the highest values among POM SC that have been reported. The moderate cycle stability of AC//$Na_6V_{10}O_{28}$ asymmetric SC in organic electrolyte is evaluated up to 1000 cycles with a retention of ~ 70 %. After the first 100 cycles the further decrease was slow with ~ 1 % per 100 cycles. These results have proofed the potential of $Na_6V_{10}O_{28}$ as promising electrodes candidates for SCs.

Experimental Section

Synthesis of $Na_6V_{10}O_{28}$

Decavanadate(V), $Na_6V_{10}O_{28}{\cdot}xH_2O$, was prepared using a literature method.[30] Decavanadate was generally obtained by acidifying an aqueous solution of vanadate, accordingly a 3 g sample of sodium metavanadate ($NaVO_3$) was dissolved in 100 mL water and 4 M HCl was used to reduce the pH to 4.8. The solution was filtered and additional HCl maintained the pH at 4.5. The bulk sodium salt of the polyanion was isolated by precipitation of the solution through the addition of 200 mL 95% ethanol. This resulted in an orange product, which was isolated by filtration and air-dried.

Characterization of $Na_6V_{10}O_{28}$

The identity of $Na_6V_{10}O_{28}$ was established by FTIR and 51V NMR. The 51V NMR measurements were performed in 5 mm tubes at 105.4 MHz, and the spectra were recorded on a 400 MHz JEOL ECX instrument. FTIR spectrophotometer (Nicolet Avatar 370) was used to detect the infrared spectra using KBr pellets. The morphology of $Na_6V_{10}O_{28}$ was characterized by field emission scanning electron microscope (FESEM, JEOL JSM 7600F), and high resolution transmission electron microscopy (HRTEM, JOEL-JSM 2100F). The Brunauer Emmetand Teller (BET) surface area and the Barrett-Joyner-Halenda (BJH) pore size distribution of $Na_6V_{10}O_{28}$ was determined by N_2 adsorption-desorption isotherms at 77 K.

Electrochemical measurement:

The active layers of electrodes were prepared by mixing active material ($Na_6V_{10}O_{28}$), poly(vinylidene fluoride) (PVDF) binder, and carbon black (super P) in N-methylpyrrolidinone (NMP) with a weight ratio of 75 : 15 : 10, respectively. Above slurry was coated onto graphite papers as working electrodes and dried at 80 °C for 10 h. An organic electrolyte (1 M $LiClO_4$ in propylene carbonate (PC)) was used as electrolyte. Cyclic voltammetry (CV) and galvanostatic charge/discharge (GCD) cycles of $Na_6V_{10}O_{28}$ working electrodes were investigated using a three-electrode cell set-up tested in a Biologic VMP3 potentiostat. Ag/$AgNO_3$ was served as the reference electrode, and platinum wire was used as the counter electrode.

The activated carbon (AC) (Norit, The Netherlands) electrode was prepared using the same method as for $Na_6V_{10}O_{28}$ electrode. The asymmetric device was fabricated using AC as positive electrode and $Na_6V_{10}O_{28}$ as negative electrode after suitable mass balance of the active materials, and porous glassy fibrous paper (GF/D) from Whatman was used as a separator. The asymmetric device was characterized by cyclic voltammetry (CV) and galvanostatic charge/discharge cycle measurements with a potentiostat (Solatron, SI 1255B) in the potential range of 0–2.8 V.

The Li-ion adsorption and vanadium bonding states of $Na_6V_{10}O_{28}$ electrodes were analyzed by X-ray photoelectron spectrometer (XPS, PHI Kratos AXIS Ultra) with a monochromatic Al Kα (1486.71 eV) X-ray radiation (15 kV/10 mA). C 1s line of the adventitious carbon at 284.6 eV was used as reference.

Acknowledgements

This work was supported by TUM CREATE which is a joint research programme between Technische Universität München (TUM) in Germany and Nanyang Technological University (NTU) in Singapore with partial funding by the National Research Foundation of Singapore.

Keywords: electrochemistry· polyoxometalates · redox chemistry · supercapacitors · materials science

[1] S. Park, K. Lian, Y. Gogotsi, *J. Electrochem. Soc.* **2009**, *156*, A921-A926.
[2] P. Simon, Y. Gogotsi, *Nat. Mater.* **2008**, *7*, 845-854.
[3] M. A. Schwegler, P. Vinke, M. Vandereijk, H. Vanbekkum, *Appl. Catal., A* **1992**, *80*, 41-57.
[4] H. Y. Lee, J. B. Goodenough, *J. Solid State Electrochem.* **1999**, *148*, 81-84.
[5] R. N. Reddy, R. G. Reddy, *J. Power Sources* **2006**, *156*, 700-704.
[6] Y. Zhang, J. Li, F. Kang, F. Gao, X. Wang, *Int. J. Hydrogen Energ.* **2012**, *37*, 860-866.
[7] K. R. Prasad, K. Koga, N. Miura, *Chem. Mater.* **2004**, *16*, 1845-1847.
[8] N. Miura, S. Oonishi, K. R. Prasad, *Electrochem. Solid-State Lett.* **2004**, *7*, A247-A249.
[9] T. Cottineau, M. Toupin, T. Delahaye, T. Brousse, D. Belanger, *Appl. Phys. A* **2006**, *82*, 599-606.
[10] A. Zolfaghari, F. Ataherian, M. Ghaemi, A. Gholami, *Electrochim. Acta* **2007**, *52*, 2806-2814.
[11] G. Wee, H. Z. Soh, Y. L. Cheah, S. G. Mhaisalkar, M. Srinivasan, *J. Mater. Chem.* **2010**, *20*, 6720-6725.
[12] U. M. Patil, S. B. Kulkarni, V. S. Jamadade, C. D. Lokhande, *J. Alloys Compound.* **2011**, *509*, 1677-1682.
[13] M. T. Pope, A. Muller, *Angew. Chem. Int. Ed.* **1991**, *30*, 34-48.
[14] U. Kortz, *Issue dedicated to Polyoxometalates, Eur. J. Inorg. Chem. 34*. 2009; Vol. 34.
[15] M. T. Pope, U. Kortz, Polyoxometalates. In *Encyclopedia of Inorganic and Bioinorganic Chemistry*, John Wiley & Sons, Ltd: 2011.
[16] M. T. Pope, A. Müller, *Polyoxometalate Chemistry: From Topology via Self-Assembly to Applications*. Kluwer Academic: Dordrecht, The Netherlands, 2001.

[17] C. L. Hill, *Special Issue on Polyoxometalates, Chem.Rev. 98*. 1998; Vol. 98.
[18] N. Kawasaki, H. Wang, R. Nakanishi, S. Hamanaka, R. Kitaura, H. Shinohara, T. Yokoyama, H. Yoshikawa, K. Awaga, *Angew. Chem. Int. Ed.* **2011**, *50*, 3471-3474.
[19] A. Yamada, J. B. Goodenough, *J. Electrochem. Soc.* **1998**, *145*, 737-743.
[20] A. M. White, R. C. T. Slade, *Electrochim. Acta* **2003**, *48*, 2583-2588.
[21] A. M. White, R. C. T. Slade, *Electrochim. Acta* **2004**, *49*, 861-865.
[22] A. K. Cuentas-Gallegos, M. Lira-Cantu, N. Casan-Pastor, P. Gomez-Romero, *Adv. Funct. Mater.* **2005**, *15*, 1125-1133.
[23] A. Cuentas-Gallegos, R. Martinez-Rosales, M. Baibarac, P. Gomez-Romero, M. E. Rincon, *Electrochem. Comm.* **2007**, *9*, 2088-2092.
[24] G. M. Suppes, C. G. Cameron, M. S. Freund, *Journal of the Electrochemical Society* **2010**, *157*, A1030-A1034.
[25] T. Akter, K. W. Hu, K. Lian, *Electrochim. Acta* **2011**, *56*, 4966-4971.
[26] V. Ruiz, J. Suarez-Guevara, P. Gomez-Romero, *Electrochem. Comm.* **2012**, *24*, 35-38.
[27] Z. Chen, V. Augustyn, J. Wen, Y. W. Zhang, M. Q. Shen, B. Dunn, Y. F. Lu, *Adv. Mater.* **2011**, *23*, 791-795.
[28] E. Frackowiak, F. Beguin, *Carbon* **2001**, *39*, 937-950.
[29] V. D. K. Zhetcheva, L. P. Pavlova, *Turk. J. Chem.* **2011**, *35*, 215-223.
[30] P. J. Domaille, *J. Am. Chem. Soc.* **1984**, *106*, 7677-7687.
[31] S. Ramos, R. O. Duarte, J. J. G. Moura, M. Aureliano, *Dalton Trans.* **2009**, 7985-7994.
[32] Z. Chen, J. J. Concepcion, M. K. Brennaman, P. Kang, M. R. Norris, P. G. Hoertz, T. J. Meyer, *Proc. Natl. Acad. Sci.* **2012**, *109*, 15606-15611.
[33] V. Aravindan, Y. L. Cheah, W. F. Mak, G. Wee, B. V. R. Chowdari, S. Madhavi, *ChemPlusChem* **2012**, *77*, 570-575.
[34] L. L. Li, S. J. Peng, Y. L. Cheah, P. F. Teh, J. Wang, G. Wee, Y. W. Ko, C. L. Wong, M. Srinivasan, *Chem. Eur. J.* **2013**, *19*, 5892-5898.
[35] J.-M. Li, K.-H. Chang, T.-H. Wu, C.-C. Hu, *J. Power Sources* **2013**, *224*, 59-65.
[36] R. S. Kalubarme, H. S. Jadhav, C.-J. Park, *Electrochim. Acta* **2013**, *87*, 457-465.
[37] F. Zhang, T. F. Zhang, X. Yang, L. Zhang, K. Leng, Y. Huang, Y. S. Chen, *Energy Environ. Sci.* **2013**, *6*, 1623-1632.
[38] M. Skunik, M. Chojak, I. A. Rutkowska, P. J. Kulesza, *Electrochim. Acta* **2008**, *53*, 3862-3869.
[39] C. Zheng, W. Qian, F. Wei, *Mater. Sci. Eng., B* **2012**, *177*, 1138-1143.
[40] A. M. White, R. C. T. Slade, *Synth. Met.* **2003**, *139*, 123-131.

Received: ((will be filled in by the editorial staff))
Published online: ((will be filled in by the editorial staff))

Entry for the Table of Contents

ARTICLES

Novel material for supercapacitors: A polyoxovanadate, $Na_6V_{10}O_{28}$, is investigated for the first time as electrode material for supercapacitors in this work. An asymmetric supercapacitor using activated carbon as positive electrode and $Na_6V_{10}O_{28}$ as negative electrode is fabricated and exhibits a high energy density of 73 Wh kg^{-1} with a power density of 312 W kg^{-1}, which successfully demonstrates that $Na_6V_{10}O_{28}$ is a promising electrode material for high energy supercapacitor applications.

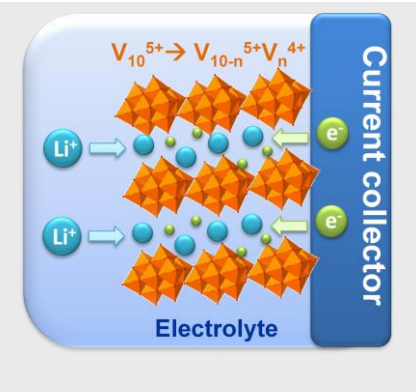

Han-Yi Chen, Grace Wee, Rami Al-Oweini, Jochen Friedl, Kim Soon Tan, Yuxi Wang, Chui Ling Wong, Ulrich Kortz, Ulrich Stimming, and Madhavi Srinivasan**

Page No. – Page No.

Polyoxovanadate as Advanced Electrode Material for Supercapacitors